Defect-Mediated Diffraction Resonances in Surface Scattering

A. Glebov, J. R. Manson,* J. G. Skofronick,† and J. P. Toennies

Max Planck Institut für Strömungsforschung, Bunsenstrasse 10, Göttingen, Germany

A new elastic surface resonance has been observed in angular distributions of He atoms scattered from a single crystal surface NaCl(001). The process has been identified as a coherent selective adsorption into one of the surface bound states followed by incoherent scattering from defects into the continuum. The reverse process has also been identified. These resonances open up possibilities for other highly defined two-dimensional elastic and inelastic surface scattering experiments. [S0031-9007(97)02364-8]

All real, clean surfaces possess a variety of intrinsic defects such as vacancies, steps, and kinks which can strongly influence the way a surface interacts with its environment. Recently, it has been shown than these surface imperfections can be characterized through a careful analysis of the weak background intensities of scattered atoms [1] or electrons [2] between the diffraction peaks. In this Letter we report on the observation of a new resonance involving elastic scattering of atoms from defects.

In the well-known resonant process of selective adsorption (SA) the incident projectile is diffracted resonantly at specified incident energies and angles into one of the bound state levels of the adsorption potential well, while still conserving its total energy [3,4]. The early work on selective adsorption was carried out using angular distributions of the total intensity without time-of-flight (TOF) energy analysis [5]. Today this method provides probably the best way for determining the bound states and the shape of the physisorption potential well near the surface [5,6]. Later, TOF methods revealed that bound state levels could also be accessed by an inelastic one phonon creation resonance [7,8] or be ejected by one phonon annihilation [8]. Recently, a related phenomena called a focused inelastic resonance (FIR) was found [9]. Here we report on a defect-mediated elastic resonance (DER) which can greatly enhance the elastic scattering from defects under conditions in which either the incident or outgoing beam is resonantly coupled to a bound state via scattering from a defect.

Since in DER the particle either enters the bound state via SA or leaves it via the reverse process of selective desorption (SD), it is useful to summarize the kinematics of these resonances [4]. A plane wave incident on a rigid periodic surface can be described by a wave vector $\mathbf{k}_i$ with components $\mathbf{K}_i$ parallel and k_{iz} perpendicular to the surface and has energy $E_i = \hbar^2 k_i^2 / 2m = \hbar^2[\mathbf{K}_i^2 + k_{iz}^2]/2m$, where m is the particle mass. Since the surface is periodic only in the parallel direction, the parallel momentum is conserved modulo a surface reciprocal lattice vector $\mathbf{G}$, while the perpendicular momentum is not conserved. Thus the allowed scattering channels will have wave vectors given by $\mathbf{k}_G = (\mathbf{K}_i + \mathbf{G}, k_{Gz})$, where the perpendicular

component is determined by conservation of energy $k_{Gz}^2 = k_i^2 - (\mathbf{K}_i + \mathbf{G})^2$. Selective adsorption bound state resonances occur whenever

$$k_{Bz}^2 = k_i^2 - (\mathbf{K}_i + \mathbf{B})^2 = -2m|\epsilon_n|\hbar^2, \qquad (1)$$

where ϵ_n is the energy of the nth bound state in the surface adsorption well and $\mathbf{B}$ is one of the $\mathbf{G}$ vectors [4]. Under the resonant conditions of Eq. (1), direct diffraction into the bound state is energetically allowed and the wave function has an amplitude component which is constrained to a bound state of the surface potential in the normal direction but parallel to the surface has a shorter wavelength than the incident wave. The nature of the wave function in the bound state is similar to the well-known Andreev two-dimensional surface states of ^{3}He on the surface of ^{4}He [10].

The high resolution helium atom scattering apparatus has been described in detail elsewhere [11]. The sum of the incident and final scattering angles is fixed at $\theta_{SD} = \theta_i + \theta_f = 90°$ and for elastic scattering the parallel wave vector transfer is given by $\Delta = [\sin(90° - \theta_i) - \sin \theta_i]$. The 6×7 mm^2 NaCl crystal target was cleaved in vacuum at scattering chamber pressures near the mid 10^{-11} torr range.

Figure 1(a) shows an overview of the total scattering intensity diffraction pattern obtained by rotating the target so as to change θ_i [and simultaneously $\theta_f = (90° - \theta_i)$] for the $\langle 100 \rangle$ azimuth. The two major diffraction peaks correspond to the surface reciprocal lattice vectors (1,1), (2,2), (−1, −1), and (−2, −2) with intensities relative to the specular peak (6×10^6 counts/s) similar to those reported previously [12]. Figure 1(b) shows the angular region ±5° on both sides of the specular on an enlarged intensity scale. The many features seen are mostly due to single phonon inelastically mediated resonances and kinematic focusing resonances [13] which are superimposed on the regular inelastic intensity from single phonon creation and annihilation. In order to remove those inelastic contributions TOF spectra were measured at angular intervals of 0.1° and only the pure elastic contribution corresponding to an energy window of about ±0.2 meV around the
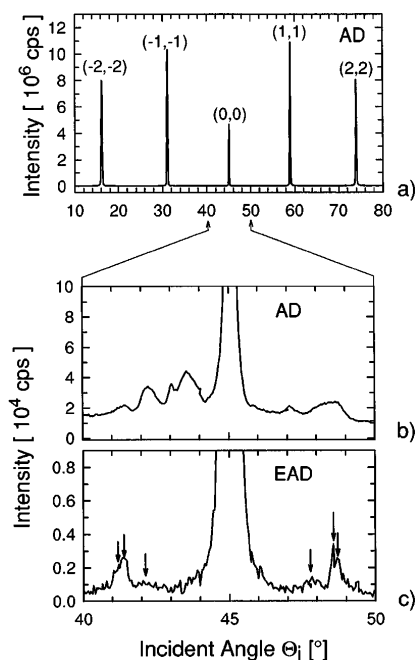
FIG. 1. Three different scattered angular distributions of He atoms with wave vector $\mathbf{k}_i = 6.55$ Å^{-1} incident on the NaCl(001) surface in the $\langle 100 \rangle$ surface azimuth: (a) total angular distribution (AD) showing the diffraction peak intensities; (b) an expanded view of the AD near the specular peak showing the diffuse background; and (c) the elastic angular distribution which contains only the elastic contribution of the TOF energy resolved spectrum.
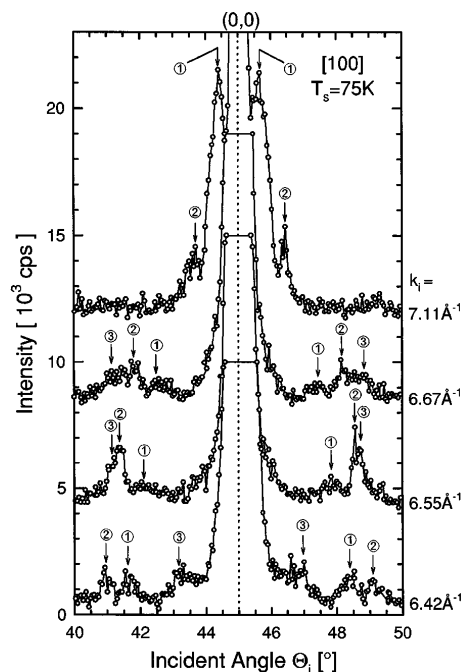

FIG. 2. Some typical EAD measurements of the diffuse elastic intensity as a function of incident angle θ_i for He incident on NaCl(001) in the $\langle 100 \rangle$ surface azimuthal direction at four different incident wave vectors $\mathbf{k}_i = 6.42$–7.11 Å. The peaks marked with numbered arrows ($\downarrow$) are the diffuse elastic resonance features. The arrow numbers 1, 2, and 3 denote the $[3(1,1)]$, $[1(2,0)]$, and $[3(-2,2)]$ resonances, respectively.

elastic peak was retained. Figure 1(c) shows the resulting elastic angular distribution (EAD), which now reveals a number of sharp DER structures with an order of magnitude lower intensity than in Fig. 1(b) superimposed on the background intensity of less than 10^3 counts/s. As discussed previously [1], this intensity is due to scattering largely from the edges of structural defects on the surface. To investigate these resonances further similar EADs were measured for 13 different incident wave vectors.

Figure 2 shows some representative EADs. In each of the scans two to three DER features are marked by arrows and the numbers 1, 2, and 3. They are symmetrically positioned about the specular peak, and the intensity of each symmetric pair is nearly equal as explained below after Eq. (2). They are clearly not diffraction features, since their positions in parallel wave vector transfer ΔK shift with incident energy, whereas any possible diffraction features would remain at fixed positions in ΔK.

Using a notation $[n(G_x, G_y)]$, where n is the number of the bound state as in Table I and G_x and G_y are the x and y components of $\mathbf{G}$ expressed in units of the NaCl surface reciprocal lattice vector of 1.58 Å^{-1}, the peaks in Fig. 2 are identified via Eq. (1) as belonging to the $[3(1,1)]$, $[1(2,0)]$, and $[3(-2,2)]$ resonances. It should be noted that the $[1(2,0)]$ and $[3(-2,2)]$ resonances are degenerate with the $[1(0,2)]$ and $[3(2,-2)]$, respectively. Note that the two resonances $[3(1,1)]$ and $[1(2,0)]$ move toward smaller values of θ_i (smaller values of parallel momentum

transfer) with increasing energy, while the $[3(-2,2)]$ resonance exhibits opposite behavior and moves to larger values of θ_i.

In Fig. 3, the open diamond shaped data points ($\diamondsuit$) show the positions of the observed DER peaks obtained from the EADs in a plot of incident angle θ_i versus incident wave vector $\mathbf{k}_i$ and the circles ($\bigcirc$) show the position of the specular diffraction peak. For comparison, the solid lines are calculated for SA conditions on the incident beam from Eq. (1), while the dashed lines are calculated from an equation similar to Eq. (1) for resonant conditions on the final scattered beam (SD), using the bound state energy levels given in Table I. These energy levels agree well with the previous measurements.

The excellent agreement of the resonance features with the calculations based on Eq. (1) establishes that the He atoms have accessed the bound states of the NaCl surface by either in the one case entering via a selective adsorption (solid lines in Fig. 3) or in the other case leaving via a selective desorption process (dashed lines in Fig. 3). Since we can rule out all inelastic processes, as well as rule out all diffraction possibilities for the second vertex required to either leave or enter the bound state, we are left with only an elastic process. The only elastic process possible is scattering from defects.

To check that indeed defects are involved, the surface defect density was intentionally reduced by baking the crystal for 12 h at a temperature of 500 K. As shown

TABLE I. Comparison of the present best fit bound state levels (ϵ_n) for NaCl(001) with previous determinations.

$-\epsilon_0$ (meV)	$-\epsilon_1$	$-\epsilon_2$	$-\epsilon_3$	Refs.
$\cdots$	3.35	$\cdots$	0.30	Present work
7.21 ± 0.10	$\cdots$	1.62 ± 0.07	0.41 ± 0.12	[13]
$\cdots$	3.7 ± 0.4	$\cdots$	$\cdots$	[5,14]
$\cdots$	3.4 ± 0.1	$\cdots$	$\cdots$	[9]
7.07 ± 0.05	$\cdots$	$\cdots$	$\cdots$	[15]
$\cdots$	4.1 ± 0.1	1.5 ± 0.1	0.31 ± 0.05	[16]

in previous studies [17], this temperature is sufficient to anneal the intrinsic surface defects of NaCl. The smoothing of the surface upon annealing resulted in a decrease of the DER peak intensities as well as the total diffuse background by a factor of 5 compared to the unannealed surface. This provides evidence that the resonances observed in the present work are mediated by intrinsic surface defects.

Figure 4(a) shows a mechanism in which the incoming beam can diffract into one of the bound states but encounters a defect while in the bound state. The defect will act as a symmetry-breaking object and can elastically scatter wave amplitudes out of the bound state in all directions. Those outwardly scattered waves which conserve total energy will appear asymptotically far from the surface as a part of the diffuse elastic amplitude. There they will interfere with the diffuse elastic signal which is directly scattered from the defect without first passing through the bound state. This interference can be described by a Feshbach resonance line shape, similarly to the case for or-

dinary selective adsorption [18]. However, if as expected the diffraction matrix element is large compared to that of the defect scattering between the continuum and bound state, then the line shape will reduce to a Lorentzian and lead to an enhancement of the diffuse elastic intensity at all final scattered angles whenever the incident beam is in resonance.

The mechanism for the reverse process also observed is shown in Fig. 4(b). A beam with wave vector $\mathbf{k}_i$ is incident at an arbitrary angle and encounters a small coverage of symmetry-breaking defects on the surface. Direct scattering from the defects will scatter partial waves into the diffuse elastic amplitude, but by the same process some amplitude will be scattered into all of the bound states, while still conserving energy. The amplitudes incoherently scattered into the bound states can subsequently leave the bound states via diffraction, but only into those diffraction states which correspond to resonance conditions. Thus Fig. 4(b) depicts a process which implies that the diffuse elastic signal due to surface defects for
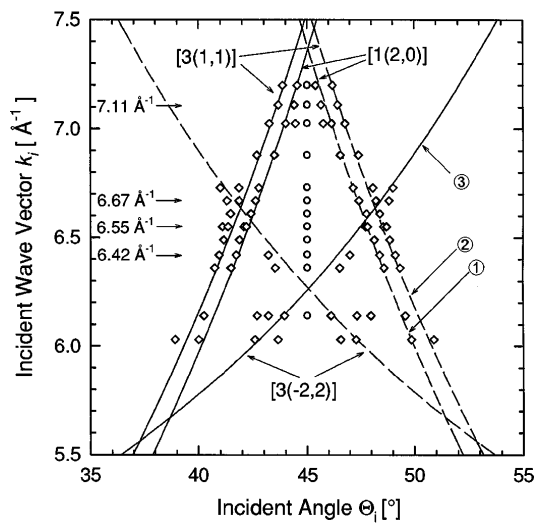

FIG. 3. Plot of the peak positions in incident angle θ_i as a function of incident total wave vector for He atom scattering on the NaCl(001)⟨110⟩. The data points shown as diamonds (◇) are the DER features, while the specular peak is marked with circles (○). The calculated curves show the expected positions of the DER features as predicted by Eq. (1), with solid curves for the process of Fig. 4(a) and dashed curves for the process of Fig. 4(b).
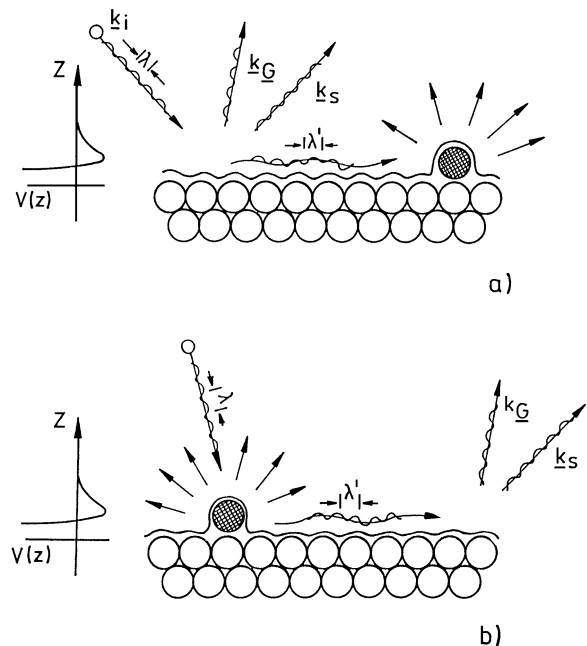

FIG. 4. Schematic representation of the forward (a) and time-reversed (b) processes that contribute to diffuse elastic resonances. Scattering into the specular and Bragg diffraction channels are marked with $\mathbf{k}_s$ and $\mathbf{k}_G$, respectively.

an incident beam of energy E_i should be enhanced in the discrete outgoing directions corresponding to bound state resonance conditions, regardless of the scattering angle of the incident beam.

The scattering matrix is invariant under time and parity reversal (TP invariance), which implies that for even parity surface potentials the two mechanisms of Figs. 4(a) and 4(b) are time-reversed images of each other. In particular, for even parity surfaces, we have the following equality in the transition matrix:

$$\langle \mathbf{k}_f |T| \mathbf{k}_i \rangle = e^{i\gamma} \langle \mathbf{k}_s |T| \mathbf{k}_{f'} \rangle, \tag{2}$$

where T is the transition operator, $\mathbf{k}_s$ is the state specular to $\mathbf{k}_i$, and $\mathbf{k}_{f'}$ is the incident state whose specular is $\mathbf{k}_f$, i.e., $\mathbf{k}_f$ and $\mathbf{k}_{f'}$ differ only in that the perpendicular components of their momenta have opposite signs. The result of interchanging final and initial angles in this in-plane fixed angle experiment is not only to change ΔK into $-\Delta K$, but also the operation $\mathbf{k}_i \rightarrow \mathbf{k}_f'$ simultaneously with $\mathbf{k}_f \rightarrow \mathbf{k}_s$. This explains why at each value of k_i in Figs. 2 and 3, pairs of peaks are symmetrically located at $\pm\Delta\theta$ on either side of the specular position at $\theta_i = 45°$ (or equivalently, at $\pm\Delta K$). For a surface with even parity, or simply even parity on average, the two symmetric peaks will have equal intensities.

The demonstration of the existence of DERs is based on the observation of the following signature effects: (i) they obey the kinematical conditions of Eq. (1) dictated by the reciprocal lattice vectors and the bound state energy levels, (ii) they appear as pairs of roughly equal intensity symmetrically positioned about the specular peak as imposed by the time-reversal symmetry of the transition matrix Eq. (2), and (iii) annealing of the surface defects leads to strong reduction of the DER peak intensities. The intensity of the DER peaks is large compared to the background because the wave in one of the bound states of the potential travels close to the surface and the probability of encountering a defect is large even if the defects are very rarefied. This is a dimensionality effect arising because the scattering into the bound state "compresses" the incoming 3D plane wave into a 2D wave traveling parallel to the surface.

Finally, we would like to discuss some future possibilities for application of the DER effect. (i) The quantitative study of DERs will enable measuring the differential and total cross sections of defects on the surface under extraordinarily well-defined conditions as a result of illumination by the two-dimensional incident wave in different selected bound states. This configuration contrasts with the usual case in which a defect is illuminated by an incident three-dimensional plane wave. (ii) There are some interesting possibilities for inelastic effects associated with DER. If DER is observed from adsorbates with low energy modes such as frustrated translation modes [19], there should be inelastic Einstein mode multiquantum overtones scattered out in all directions by the defect according to the processes of Fig. 4(a). We would expect the bound state incident wave to impart large parallel momentum transfers and hence have large inelastic intensities. (iii) The DER is not limited to atom or molecule scattering, it should also be observed in electron scattering or any other scattering process where one can observe selective adsorption type resonances [20,21].

*Permanent address: Department of Physics and Astronomy, Clemson University, Clemson, SC 29634.

†Permanent address: Department of Physics, Florida State University, Tallahassee, FL 32306.

[1] A. M. Lahee, J. R. Manson, J. P. Toennies, and Ch. Wöll, Phys. Rev. Lett. **57**, 471 (1986); W. A. Schlup and K. H. Rieder, Phys. Rev. Lett. **56**, 73 (1986).

[2] For example, M. Henzler, in *Electron Spectroscopy for Surface Analysis,* edited by H. Ibach (Springer, Berlin, 1977).

[3] R. Frisch and O. Stern, Z. Phys. **84**, 430 (1933).

[4] J. E. Lennard-Jones and A. F. Devonshire, Proc. R. Soc. (London) **156**, 6 (1936); **158**, 242 (1937).

[5] H. Hoinkes, Rev. Mod. Phys. **52**, 933 (1980).

[6] H. Hoinkes and H. Wilsch, in *Helium Atom Scattering from Surfaces,* edited by E. Hulpke (Springer-Verlag, Berlin, 1992), p. 113.

[7] G. Brusdeylins, R. B. Doak, and J. P. Toennies, J. Chem. Phys. **75**, 1784 (1981).

[8] G. Lilienkamp and J. P. Toennies, J. Chem. Phys. **78**, 5210 (1983).

[9] G. Benedek, R. Gerlach, A. Glebov, G. Lange, S. Miret-Artés, J. G. Skofronick, and J. P. Toennies, Phys. Rev. B **53**, 11 211 (1996).

[10] A. F. Andreev, Zh. Eksp. Teor. Fiz. **50**, 1415 (1966) [Sov. Phys. JETP **23**, 939 (1966)].

[11] J. P. Toennies and R. Vollmer, Phys. Rev. B **44**, 9833 (1991).

[12] L. W. Bruch, A. Glebov, J. P. Toennies, and H. Weiss, J. Chem. Phys. **103**, 5109 (1995).

[13] G. Benedek, G. Brusdeylins, R. Bruce Doak, J. G. Skofronick, and J. P. Toennies, Phys. Rev. B **28**, 2104 (1983).

[14] J. R. Bledsoe, Univ. of Virginia, Report No. AEEP-3719-101-72U (unpublished).

[15] G. Benedek, A. Glebov, W. Silvestri, J. Skofronick, and J. P. Toennies, Surf. Sci. (to be published).

[16] W. Y. Leung, J. Z. Larese, and D. R. Frankl, Surf. Sci. **143**, L398 (1984).

[17] H. Höche, J. P. Toennies, and R. Vollmer, Phys. Rev. B **50**, 679 (1994).

[18] J. R. Manson, *Helium Atom Scattering from Surfaces* (Ref. [6]), p. 173.

[19] F. Hofmann and J. P. Toennies, Chem. Rev. **96**, 1307 (1996).

[20] E. G. McRae, Rev. Mod. Phys. **51**, 541 (1979).

[21] M. Rocca and F. Moresco, Phys. Rev. Lett. **73**, 822 (1994).